Macromolecular Research

Note

DOI 10.1007/s13233-018-6138-5

www.springer.com/13233 pISSN 1598-5032 eISSN 2092-7673

Effect of Ozone Treatment on Fracture Toughness of Single-Walled Carbon Nanotubes-Reinforced Epoxy Resin Initiated by a Thermal Latent Catalyst

Min-Joo Kang[1]
Fan-Long Jin[2]
Soo-Jin Park*[,1]

[1] Department of Chemistry, Inha University, 100 Inharo, Incheon 22212, Korea
[2] Department of Polymer Materials, Jinlin Institute of Chemical Technology, Jilin City 132022, P. R. China

Received December 11, 2017 / Revised April 24, 2018 / Accepted May 21, 2018

1. Introduction

An increasing number of studies on filler-reinforced composites with carbon materials have been recently reported.[1,2] Composites based on epoxy resins are widely used as industrial materials, and epoxy resins, such as the diglycidylether of bisphenol A (DGEBA), are the most ubiquitous type of thermosetting polymers.[3] In particular, epoxy resins are extensively applied in engineering and used in various industrial applications such as adhesives, electronics, and coatings. This is because of their excellent mechanical and chemical properties, including high tensile and compressive strengths, good solvent resistance, outstanding chemical resistance, and high heat-distortion temperatures.[4,5] However, after curing, epoxy resins become brittle owing to their high cross-linking density. To compensate for this disadvantage, other materials such as inorganic particles and thermoplastic polymers have been added to the composite.[6,7]

Single-walled carbon nanotubes (SWCNTs) have demonstrated remarkable mechanical and physical properties owing to their structure, size, and topology. They are highly promising for use in various applications, including in nanotube-reinforced materials for nanocomposites and nanoelectronic devices.[8-14] Although SWCNTs have great potential, their use has been limited for the processing of systems that require optimization to obtain uniform dispersion, controlled interfacial properties, and specific orientation in the composite. Therefore, advanced processes to deal with SWCNTs must be developed to overcome these problems.

Ozone treatment as a dry oxidation method is one of the most common techniques used in industry and introduces various oxygen functional groups such as -C=O, -COOH, and -OH, to the surface of the materials. The increased number of oxygen-containing functional groups on surface of SWCNTs can improve the interfacial interaction between filler and epoxy resins, thereby improving the mechanical and physical properties of the resulting composite.[15-21]

Acknowledgments: This work was supported by the Leading Human Resource Training Program of Regional Neo industry through the National Research Foundation of Korea (NRF) funded by the Ministry of Science, ICT and future Planning (NRF-2016H1D5A1909732) and the Korea Institute of Energy Technology Evaluation and Planning (KETEP) and the Ministry of Trade, Industry & Energy (MOTIE) of the Republic of Korea (20153030031710).

***Corresponding Author:** Soo-Jin Park (sjpark@inha.ac.kr)

Generally, amines or anhydrides are used as a curing agent, the addition of which is a prerequisite for the thermal curing of epoxy resins.[22] The development of thermal latent initiators for epoxy resins has attracted considerable attention because amines and anhydrides have many drawbacks, including high toxicity and low storage stability.[23] The development of efficient thermal latent initiators is desirable for improving the handling and storage stability of epoxy resins,[24] and the initiators must be activated by external stimulation such as heat and light.[25] Therefore, a thermal latent initiator can easily control the initiation and curing of an epoxy system.[26] Several types of catalysts, such as sulfonium, pyrazinium, and ammonium salts, with few nucleophilic counteranions, and counterions of thermal latent initiators are generally inorganic metal halide complex anions, such as BF_3^- ether, BF_3^- amine, or SbF_6^-.[27]

In this study, the SWCNTs used as a reinforcing agent were treated with ozone, and *N*-benzylpyrazinium hexafluoroantimonate (BPH) was synthesized as a thermal latent initiator. In addition, DGEBA/SWCNT composites were fabricated, and their mechanical interfacial properties were examined by fracture testing.

2. Experimental

2.1. Materials

The epoxy resin used in this study was commercially available DGEBA (YD-128, Kukdo Chemical Co). The epoxide equivalent weight of DGEBA was 185-190 g/equiv, and the density was 1.16 g/cm^3 at 25 °C. The SWCNTs used as a filler with a diameter of 1.6±0.4 nm were obtained (Ocsial Co.). To synthesize BPH, organic starting materials such as pyrazine ($C_4H_4N_2$), benzyl bromide (C_7H_7Br), and sodium hexafluoroantimonate ($NaSbF_6$) were obtained from Aldrich Chemical Co., and acetonitrile, diethyl ether, and methanol were used as solvents for the filtration and purification (Daejung Chemical and Metals Co.).

2.2. Ozone treatment of SWCNTs

Ozone was produced from oxygen gas using an ozone generator (OzoneTechLabII), with the power parameters set to 220 V and 60 Hz. Ozone was produced at 5 g/h under 0.05 MPa with a gas flow of 0.5 L/min. The ozone treatment was performed for 6 h at room temperature. The ozone-treated SWCNTs are referred to as O-SWCNTs.

2.3. Synthesis of BPH

A solution of pyrazine (10 g, 0.12 mol) in acetonitrile (50 mL) was added to benzyl bromide (22.23 g, 0.13 mol) at 25 °C. After stirring the mixture for 3 days, the precipitated solid was collected by filtration and washed with ether. The solid product was subsequently evaporated in a vacuum oven. After sufficient evaporation, the obtained product was added to a solution of $NaSbF_6$ at the same molar ratio as the product in deionized water, and the mixture was stirred for 10 min. The product was filtered with ether and dried in a vacuum oven. Finally, the product was recrystallized from methanol, yielding a white solid.[28,29]

FTIR (cm^{-1}, KBr): 3116 (N-H), 1445 (C=C), 1356 (C-N), 1157, 756, 705, and 654 (C-H).

^1H NMR (ppm, acetone-d_6): 9.637-9.648 (pyridine ring), 9.356-9.363 (pyridine ring), 7.518-7.737 (aromatic ring), and 6.212 (-CH_2-).

Elemental analysis ($C_{11}H_{11}N_2SbF_6$): Calculated C: 32.45%, H: 2.70%, and N: 6.88%. Found C: 32.43%, H: 2.58%, and N: 6.78%.

2.4. Fabrication of epoxy-based composites

The composites were prepared with different ratios of SWCNTs and O-SWCNTs (0.10, 0.25, and 0.50 wt%), and were fabricated by the following processes. The SWCNTs and O-SWCNTs were dispersed separately in acetone by sonication at room temperature for 1 h. The solution was added to the epoxy resins and mixed by stirring at 80 °C for 1 h. The mixture was placed on a hot plate for 24 h at 100 °C to completely remove the solvent. Thereafter, BPH was added in the mixture and stirred for at 80 °C for 1 h. The final mixture was placed in a vacuum oven for 30 min at 60 °C to remove bubbles and then cured at 170 °C for 1 h, 200 °C for 2 h, and 230 °C for 1 h in a convection oven.

2.5. Characterization and measurements

The morphologies of the SWCNTs were observed using scanning electron microscopy (SEM, Hitachi SU8010) and field-emission transmission electron microscopy (FE-TEM, Jeol JEM-2100F).

The surface properties of the SWCNTs and O-SWCNTs were investigated using a Fourier transform-infrared vacuum spectrometer (FTIR, Bruker Vertex 80V) and X-ray photoelectron spectroscopy (XPS, Thermo K-Alpha).

The chemical structure of BPH was characterized using FTIR, nuclear magnetic resonance (^1H NMR, Bruker Avance III), and elemental analysis (EA, Thermo EA1112).

The glass transition temperature (T_g) of the DGEBA/SWCNT and DGEBA/O-SWCNT composites were measured using a dynamic mechanical analyzer (DMA Q800, TA Instruments) from 30 to 250 °C, a heating rate of 4 °C/min, and a frequency of 1 Hz. The sample dimensions were 2 mm × 5 mm × 20 mm.

The fracture toughness tests were performed according to ASTM E399 using a three-point bending test on a universal testing machine (UTM, Lloyd LR5K). The sample dimensions were 5 mm×10 mm×50 mm, including a single edge notch (SEN), and the cross-head speed was 10 mm/min.

SEM was used to investigate the morphologies of the fractured surfaces after the fracture tests.

3. Results and discussion

Figure 1 shows the surface morphology of the SWCNTs used in this study, which exhibited smooth surfaces approximately 1.6 nm in diameter.

The surface properties of the SWCNTs and O-SWCNTs were examined using FTIR and XPS. Figure 2(a) shows the FTIR spectra of the SWCNTs and O-SWCNTs. Characteristic absorption peaks observed at 2844-2920 and 1645 cm^{-1} were attributed to the C-H and C=C groups, respectively, which decreased in intensity after the ozone treatment. After the ozone treatment, the peaks corresponding to the C=O, C-OH, and C-O groups at 1531, 1379, and 1137 cm^{-1}, respectively, increased and broadened. This indicated that oxygen-containing functional groups were introduced onto the SWCNTs surfaces by the ozone treatment.[30,31]

Figure 2(b) shows the XPS spectra of the SWCNTs and O-SWCNTs. Characteristic peaks of C=C, C-C, C-O, and C=O were observed at 283.9, 284.7, 286.0, and 287.7 eV, respectively. The peaks corresponding to C=C and C-C decreased after ozone treatment, while those of C-O and C=O increased in intensity.[17,18,32] These results demonstrate that oxygen-containing functional groups were introduced onto the surface of the nanotubes after ozone treatment.

The T_g value of the DGEBA/SWCNT and DGEBA/O-SWCNT composites was obtained from the DMA spectra, and the results are summarized in Table 1. The T_g value of the composites decreased with increasing SWCNT or O-SWCNT content compared to that of neat epoxy. This was likely due to the interfacial interactions between the carbon nanotubes and epoxy matrix in the composites.[33]

The mechanical interfacial properties of the DGEBA/SWCNT and DGEBA/O-SWCNT composites were investigated using

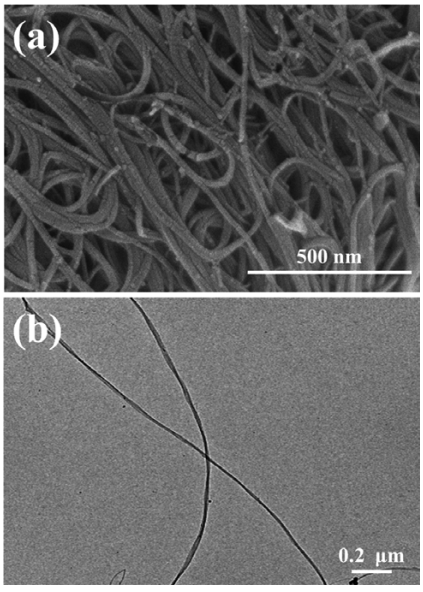

Figure 1. (a) SEM and (b) TEM images of SWCNTs.

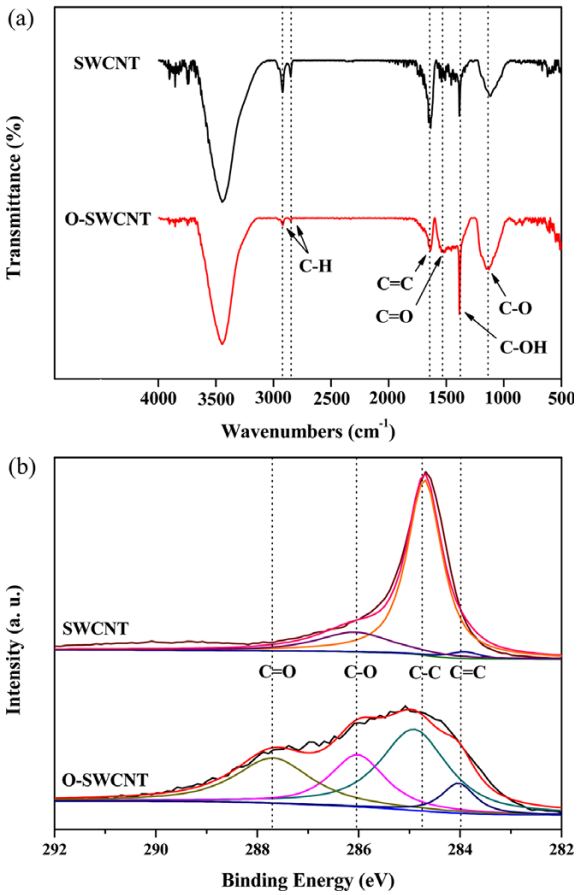

Figure 2. (a) FTIR and (b) XPS spectra of SWCNTs and O-SWCNTs.

Table 1. Glass transition temperature of the DGEBA/SWCNT and DGEBA/O-SWCNT composites obtained from DMA

No.	SWCNT	O-SWCNT	T_g (°C)
1	0	0	119.8
2	0.1	0	118.2
3	0.25	0	108.7
4	0.5	0	96.1
5	0	0.1	119.0
6	0	0.25	110.7
7	0	0.5	97.8

fracture toughness measurements. The critical stress intensity factor (K_{IC}) and critical strain energy release rate (G_{IC}) were calculated as the key fracture toughness parameters using the following equations:[34-36]

$$K_{IC} = \frac{P \cdot L}{b d^{3/2}} Y \quad (1)$$

$$Y = \frac{3a/d^{1/2}[1.99 - (a/d)(1-a/d)(2.15 - 3.93a/d + (2.7a^2)/b^2)]}{2(1+2a/d)(1-a/d)^{3/2}} \quad (2)$$

$$G_{IC} = \frac{(1-v^2) \cdot K_{IC}^2}{E} \quad (3)$$

where a is the pre-crack length (mm), b is the specimen width (mm), d is the specimen thickness (mm), P is the critical load for crack propagation, L is the length of the span (mm), v is Poisson's ratio (0.3), and E is the tensile modulus acquired from fracture testing.

Figure 3(a) shows the K_{IC} values of DGEBA/SWCNT and DGEBA/O-SWCNT composites. The K_{IC} values of the DGEBA/SWCNT and DGEBA/O-SWCNT composites increased with the increasing SWCNTs/O-SWCNTs content to 0.10 wt% and decreased thereafter. The DGEBA/SWCNT composite containing 0.10 wt% SWCNTs exhibited a K_{IC} value of 2.99 MPa $m^{1/2}$, which was 20% higher than that of the neat epoxy resins. The K_{IC} of the DGEBA/O-SWCNT composite with 0.10 wt% O-SWCNTs was 4.13 MPa $m^{1/2}$, which was 66% higher than that of neat epoxy resins and 38% higher than that of the DGEBA/SWCNT composite. The ozone treatment introduces various oxygen-containing functional groups onto the SWCNT surfaces. These functional groups enhance the interfacial interaction between the nanotubes and epoxy matrix, thereby improving their mechanical interfacial properties. Notably, the mechanical properties deteriorated when more than 0.10 wt% O-SWCNTs was added. This was likely because the carbon nanotubes were easily aggregated at high O-SWCNT contents and the compatibility between the O-SWNTs and epoxy matrix subsequently worsened, resulting in deteriorating mechanical interfacial properties.

Figure 3(b) shows the G_{IC} values of DGEBA/SWCNT and DGEBA/O-SWCNT composites. The G_{IC} values of the DGEBA/SWCNT and DGEBA/O-SWCNT composites increased with increasing SWCNT/O-SWCNT content to 0.10 wt% and decreased thereafter. The DGEBA/SWCNT composite containing 0.10 wt% SWCNTs exhibited a G_{IC} value of 8.31 kJ/m^2, which was 48% higher than

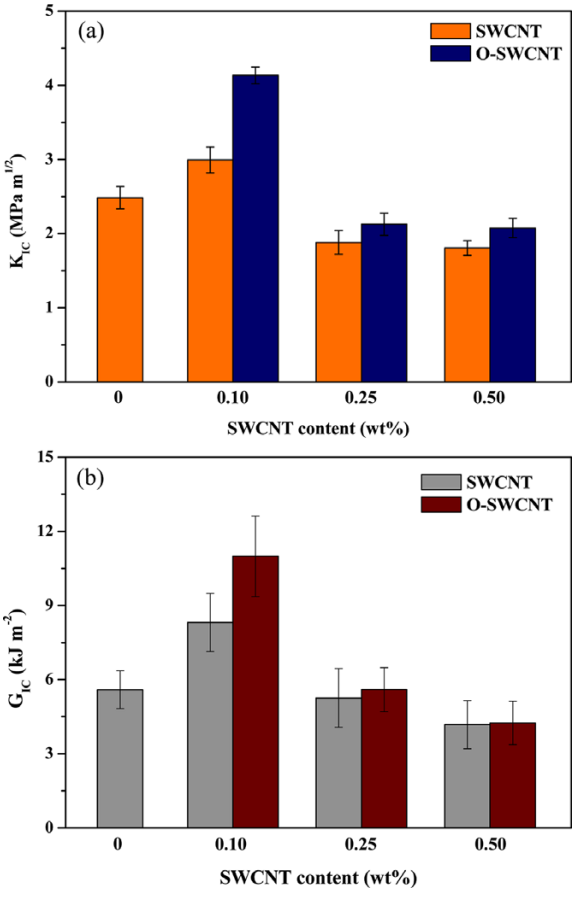

Figure 3. Mechanical properties of DGEBA/SWCNT and DGEBA/O-SWCNT composites: (a) K_{IC} and (b) G_{IC}.

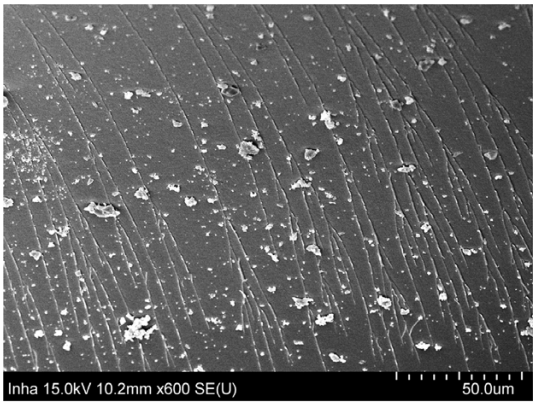

(a)

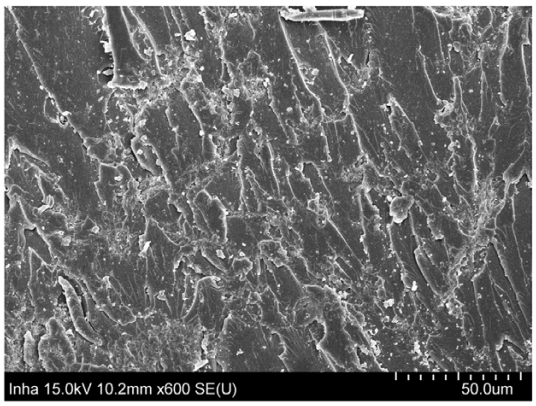

(b)

Figure 4. SEM images of the cross-sectional fracture surfaces of (a) neat DGEBA and (b) 0.10 wt% DGEBA/O-SWCNT composite (magnification of 600).

that of neat epoxy resins. The G_{IC} of DGEBA/O-SWCNT composite with 0.10wt% O-SWCNTs was 10.98 kJ/m^2, which was 96% higher than that of neat epoxy resins and 32% higher than that of the DGEBA/SWCNT composite.

The surface morphologies of the neat epoxy resins and DGEBA/O-SWCNT composite were investigated after the fracture tests, and are shown in Figure 4. The SEM micrograph of neat DGEBA exhibited a relatively smooth surface (Figure 4(a)). In contrast, the cracks in the DGEBA/O-SWCNT composite were rougher and far more pervasive than those in neat DGEBA (Figure 4(b)). The rough surfaces were generated because a significant amount of energy was required during crack propagation.

4. Conclusions

SWCNTs were treated with ozone to introduce oxygen-containing functional groups onto their surfaces. Subsequently, SWCNT-reinforced epoxy composites were prepared using BPH as a thermal latent initiator, and their mechanical interfacial properties were investigated. Fracture toughness of the DGEBA/O-SWCNT composites was significantly higher than that of neat epoxy resins or DGEBA/SWCNT composites. This improvement could be attributed to the superior dispersion of O-SWCNTs in the epoxy matrix originating from the improved interfacial interactions between oxygen-containing functional groups on the O-SWCNT surface and epoxy matrix.

References

(1) S. Stankovich, D. A. Dikin, G. H. Dommett, K. M. Kohlhaas, E. J. Zimney, E. A. Stach, R. D. Piner, S. T. Nguyen, and R. S. Ruoff, *Nature*, **442**, 282 (2006).
(2) A. C. Balazs, T. Emrick, and T. P. Russell, *Science*, **314**, 1107 (2006).
(3) J. Wan, Z. Y. Bu, C. J. Xu, B. G. Li, and H. Fan, *Thermochim. Acta*, **519**, 72 (2011).
(4) S. J. Park, G. Y. Heo, and D. H. Suh, *J. Polym. Sci., Part A: Polym. Chem.*, **41**, 2393 (2003).
(5) Y. R. Ham, D. H. Lee, S. H. Kim, Y. J. Shin, M. Yang, and J. S. Shin, *J. Ind. Eng. Chem.*, **16**, 728 (2010).
(6) M. C. Chen, D. J. Hourston, F. U. Schafer, and T. N. Huckerby, *Polymer*, **36**, 3287 (1995).
(7) B. D. Che, L. T. T. Nguyen, B. Q. Nguyen, H. T. Nguyen, T. Van Le, and N. H. Nguyen, *Macromol. Res.*, **22**, 1221 (2014).
(8) A. A. Azeez, K. Y. Rhee, S. J. Park, and D. Hui, *Compos. Part B: Eng.*, **45**, 308 (2013).
(9) F. H. Gojny, M. H. Wichmann, B. Fiedler, I. A. Kinloch, W. Bauhofer, A. H. Windle, and K. Schulte, *Polymer*, **47**, 2036 (2006).
(10) M. J. Treacy, T. W. Ebbesen, and J. M. Gibson, *Nature*, **381**, 678 (1996).
(11) E. W. Wong, P. E. Sheehan, and C. M. Lieber, *Science*, **277**, 1971 (1997).
(12) P. Poncharal, Z. L. Wang, D. Ugarte, and W. A. De Heer, *Science*, **283**, 1513 (1999).
(13) R. Kamalakaran, M. Terrones, T. Seeger, P. Kohler-Redlich, M. Rühle, Y. A. Kim, T. Hayashi, and M. Endo, *Appl. Phys. Lett.*, **77**, 3385 (2000).
(14) Z. Jin, Z. Zhang, and L. Meng, *Mater. Chem. Phys.*, **97**, 167 (2006).
(15) H. Valdés, M. Sánchez-Polo, J. Rivera-Utrilla, and C. A. Zaror, *Langmuir*, **18**, 2111 (2002).
(16) D. B. Mawhinney, V. Naumenko, A. Kuznetsova, J. T. Yates, J. Liu, and R. E. Smalley, *J. Am. Chem. Soc.*, **122**, 2383 (2000).
(17) S. J. Park and S. Y. Jin, *J. Colloid Interface Sci.*, **286**, 417 (2005).
(18) S. J. Park and B. J. Kim, *Mater. Sci. Eng. Part A: Struct.*, **408**, 269 (2005).
(19) J. Yuan, L. P. Ma, S. Pei, J. Du, Y. Su, W. Ren, and H. M. Cheng, *ACS Nano*, **7**, 4233 (2013).
(20) Z. Xu, M. Yue, L. Chen, B. Zhou, M. Shan, J. Niu, B. Li, and X. Qian, *Chem. Eng. J.*, **240**, 187 (2014).
(21) D. C. Vennerberg, R. L. Quirino, Y. Jang, and M. R. Kessler, *ACS Appl. Mater. Interfaces*, **6**, 1835 (2014).
(22) S. J. Park, F. L. Jin, and J. R. Lee, *Macromol. Rapid Commun.*, **25**, 724 (2004).
(23) K. Morio, H. Murase, H. Tsuchiya, and T. Endo, *J. Appl. Polym. Sci.*, **32**, 5727 (1986).
(24) S. J. Park, T. J. Kim, and J. R. Lee, *J. Polym. Sci., Part B: Polym. Phys.*, **38**, 2114 (2000).
(25) S. J. Park, M. K. Seo, J. R. Lee, and D. R. Lee, *J. Polym. Sci., Part A: Polym. Chem.*, **39**, 187 (2001).
(26) Y. C. Kim, S. J. Park, and J. R. Lee, *Polym. J.*, **29**, 759 (1997).
(27) S. J. Park and F. L. Jin, *Polym. Degrad. Stab.*, **86**, 515 (2004).
(28) S. J. Park, F. L. Jin, J. R. Lee, and J. S. Shin, *Eur. Polym. J.*, **41**, 231 (2005).
(29) S. J. Park, G. Y. Heo, J. R. Lee, S. Y. Shim, and D. H. Suh, *Polym. Korea*, **25**, 558 (2001).
(30) A. Cohen, Q. L. Yan, A. Shlomovich, A. Aizikovich, N. Petrutik, and M. Gozin, *RSC Adv.*, **5**, 106971 (2015).
(31) S. Y. Shen, J. C. Chen, S. H. Liu, R. H. Chang, H. J. Liaw,and C. M. Shu, *J. Thermanal. Calorim.*, **113**, 1619 (2013).
(32) P. Cools, E. Sainz-García, N. D. Geyter, A. Nikiforov, M. Blajan, K. Shimizu, F. Alba-Elías, C. Leys, and R. Morent, *Plasma Process. Polym.*, **12**, 1153 (2015).
(33) K. S. Khare and R. Khare, *J. Phys. Chem. B*, **117**, 7444 (2013).
(34) L. C. Tang, Y. J. Wan, D. Yan, Y. B. Pei, L. Zhao, Y. B. Li, L. B. Wu, L. X. Jiang, and G. Q. Lai, *Carbon*, **60**, 16 (2013).
(35) K. E. Choi and M. K. Seo, *Carbon Lett.*, **14**, 58 (2013).
(36) R. Wang, Z. Li, W. Liu, W. Jiao, L. Hao, and F. Yang, *Compos. Sci. Technol.*, **87**, 29 (2013).

